Airfoil Boundary-Layer Response to an Unsteady Turbulent Flowfield

Robert W. Renoud* and Richard M. Howard†
U.S. Naval Postgraduate School, Monterey, California

The time-dependent boundary-layer response to a periodic turbulent flowfield has been studied for attached flow over an airfoil at laminar, transitional, and turbulent conditions. Hot-wire velocity measurements were made for nonstationary mean velocity and turbulence intensity profiles and for power spectra and cumulative power spectra plots. After the initial passage of the highly turbulent pulse, the boundary layer recovers to the undisturbed transitional or turbulent state through a recovery period marked by a reduced thickness, a decreased level of turbulence below that of the undisturbed state, and a turbulence power level orders of magnitude less than the undisturbed state. Use of a spinning rod as a turbulence-generating device indicates that the effect causing this laminarization is not the thrusting-propeller effect considered in earlier tests. A commonly used acceleration parameter is applied to the time-dependent flow and correlates well. Further work will consider the effect on flows near separation.

Nomenclature

F_c = filter cutoff frequency
K = acceleration parameter, Eq. (1)
Re_θ = momentum-thickness Reynolds number
Tu = turbulence intensity; the mean square of the fluctuating velocity component in the streamwise plane, normalized by the boundary-layer edge velocity
U = local streamwise mean velocity
x = streamwise coordinate
y = coordinate normal to the airfoil surface
ν = kinematic viscosity

Introduction

In many instances, the boundary layer on a wing may be sensitive to disturbances in the flow environment. Examples include airfoil performance degradation due to contamination by insects, rain, or ice; the interference of shed tip vortices on a helicopter rotor blade; and the high turbulence levels found in turbomachinery.

The effects of steady disturbances have been studied to a great extent; unsteady effects have been treated to a much lesser degree. Most studies of an unsteady flowfield involve either a pitching airfoil, related to the dynamic stall phenomenon, or a streamwise velocity variation, usually sinusoidal, over a stationary airfoil. A review of the former is given by Carr,[1] and a recent study of the latter is described by Brendel.[2] In both of these cases, it is a variation of the mean or inviscid flowfield that characterizes the flow condition. What is considered here is the response of a wing boundary layer to a periodically varying turbulent disturbance in a mean flow. Unsteady turbulent flowfields of interest may in practice be periodic, such as the propeller slipstream over an aircraft wing; or they may be single-event occurrences, such as a wind gust or control surface disturbance. In either case, one method to study the effects of such a flowfield is by high-speed data acquisition and ensemble-averaging of periodic data for a characterization of the boundary-layer response.

Previous work in this area by Miley et al.[3] and by Howard and Miley[4] treated the propeller slipstream flowfield over a laminar wing boundary layer. In those tests, thrusting and freewheeling propeller wakes were the input disturbances. It is desirable to consider a more generic source of periodic turbulence that has a greater application to single-event disturbances. This type of disturbance is of concern for a maneuvering aircraft, the lifting surface of which may penetrate the wake of a second aircraft, a launched missile, or a canard control surface.

The result of such a disturbance may be particularly important for an aircraft operating near stall or in the post-stall flight regime during aggressive maneuvering; a change in the wing boundary layer behavior may potentially affect the ability of the flow to remain attached during the maneuver, and a loss of lift over one of the lifting surfaces could adversely affect the control of the aircraft. The use of large-deflection control surfaces at low speeds and of dynamic stall for augmented lift, and the possible operation at poststall flight angles of attack, require enhanced configurational aerodynamics in the design of the advanced fighter aircraft. The effect of single-event freestream disturbances at supermaneuvering conditions is largely unknown.

This work considers the effect of a periodic disturbance on attached flows for laminar, transitional, and turbulent boundary layers; future work will treat the case of flows near separation.

Experimental Investigation

Wind Tunnel and Model

Tests were performed in the low-speed wind tunnel at the Naval Postgraduate School. This wind tunnel is of the closed-return type with a 0.8-m by 1.0-m test section; the height of the test section is further reduced to 0.7 m by the addition of a reflection plane (hereafter referred to as the "floor"). A 0.61-m wide, 0.25-m chord airfoil model was supported between vertical plates running from the floor to the ceiling. The airfoil used was from a helicopter tail rotor, filled to contour and refinished. The airfoil contour is shown in Fig. 1; the coordinates can be found in Ref. 5.

A 9.5-mm-diam polished steel rod that was 0.41 m long was rotated 10% chord distance upstream of the wing leading edge, with the axis of rotation 25% chord distance below the

Received April 14, 1988; revision received Nov. 28, 1989.

*Graduate Student; currently Chief of Avionics Branch, Aircraft Repair and Supply Center, U.S. Coast Guard, Elizabeth City, NC. Member AIAA.

†Assistant Professor, Department of Aeronautics and Astronautics. Member AIAA.

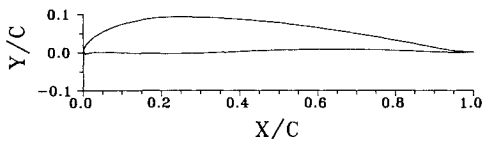

Fig. 1 Airfoil.

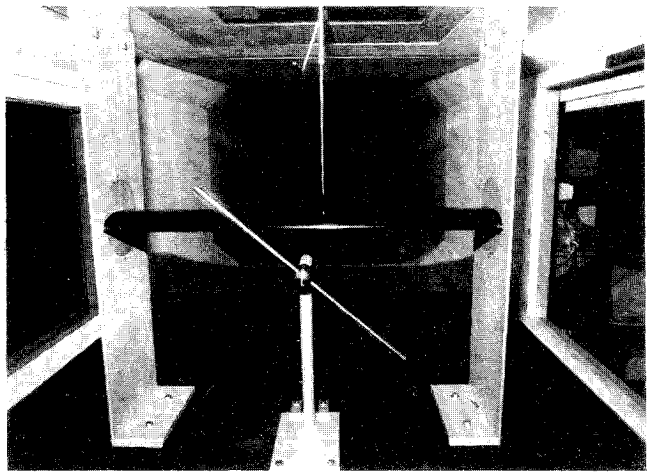

Fig. 2 Wind tunnel model and rotating assembly.

chordline. The rod was rotated at a speed of 25 Hz. The rod was turned through a flexible shaft that was held in place at the rod end by a vertical support attached to the floor. An electric motor situated behind and below the airfoil assembly behind the reflection plane turned the flexible shaft. The airfoil and spinning rod arrangement is shown in the test section in Fig. 2.

The nominal tunnel velocity was maintained at 29 m/s for a chord Reynolds number of 5×10^6. The ambient turbulence intensity at this tunnel speed was 0.18%. The Reynolds number of the spinning rod varied from about 2×10^4 near the hub to 2.8×10^4 at the tip.

Hardware

A three-dimensional traversing mechanism mounted on top of the test section was used to position the hot-wire probe at 30, 50, and 70% chord positions and to move the sensor throughout the boundary layer. It was desired to observe the time-dependent boundary-layer response in naturally laminar, transitional, and turbulent boundary layers, and the amount of data necessary for resolution and ensemble averaging only allowed for the three positions to be considered. The traverser was controlled by a microcomputer, with an available step size of 0.0032 mm. Probe locations, hot-wire velocity data, and a two-per-revolution signal generated by a proximity transducer were recorded by a microcomputer.

A single-sensor hot-wire was traversed through the boundary layer from a position near the wing surface to the external flow. The wire was positioned to within 0.081 mm of the surface by sighting the magnified image of the sensor and its reflected image in the wing surface through an engineer's transit.

Data were recorded at 50 kHz through a high-speed data acquisition board in a microcomputer using commercial data acquisition software. Because of the reading and storage requirements of the software, all data were processed after storage. This procedure resulted in simple data acquisition but also in the requirement of storing 50 MB of data for each boundary-layer location. Forty-five turbulent pulses (passes of the rod wake) were recorded for ensemble-averaging of instantaneous

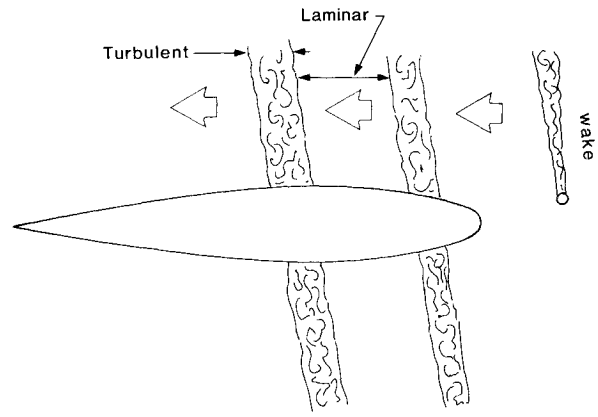

Fig. 3 Turbulence disturbance flow model.

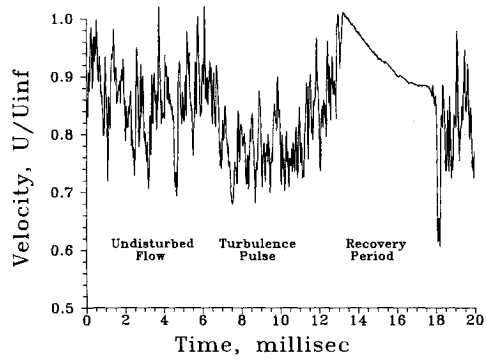

Fig. 4 Raw data, one turbulent pulse, near surface, 70% chord.

velocity and turbulence intensity profiles. For a discussion of the sufficiency of 45 to 50 pulses, see Ref. 6.

Experimental Procedure

A single angle of attack was considered in the wind tunnel tests. The angle of attack was set to zero based on chord line, and no upflow correction was applied. The purpose of the present study was to investigate the wing boundary-layer behavior for attached flows; future work will include an investigation near stall at a condition of incipient separation. Hot-wire calibrations were conducted before and after each run; rotational speed was kept within 0.5 Hz of 25 Hz.

Results

Sample Case

Figure 3 shows a simple two-dimensional model of the flow considered. The wake from the rod is convected downstream and passes over the wing surface in a periodic manner. Though the flowfield is three-dimensional, a quasi-two-dimensional approach is being considered. Crossflow components were investigated in an earlier study[6]; the crossflow velocity component was found to be about 10% of the streamwise mean. Most noticeable in the time-dependent traces was the indication of the vortex. As the crossflow components, though not negligible, were much smaller than the streamwise components, it was decided to investigate the model as shown in a two-dimensional model for a basic understanding of the effect on the streamwise boundary layer.

Figure 4 gives a typical velocity response for a single pulse, here at 70% chord. The hot-wire sensor is very near the wing surface. Because of the changing edge value of velocity with time, the local velocity has been made dimensionless by the freestream value. The "undisturbed flow" represents the naturally turbulent boundary layer existing at this chord position. The "turbulence pulse" shows the velocity deficit due to the

pulse passage with a continued high level of turbulence. The "recovery period" shows an unusual behavior after the pulse passes as the flow returns to the undisturbed state. The time of the pulse passage is 20 ms. The nature of the recovery period will be discussed in detail later. It should be mentioned that this behavior has been observed in flight on a light twin-engine aircraft at varying thrust conditions, on a single-engine aircraft at idle throttle, on a freewheeling propeller/wing-glove arrangement, and in the wind tunnel with various propellers and a wing model. Except for the thrusting characteristics accelerating the flowfield, the general behavior has been nearly identical.

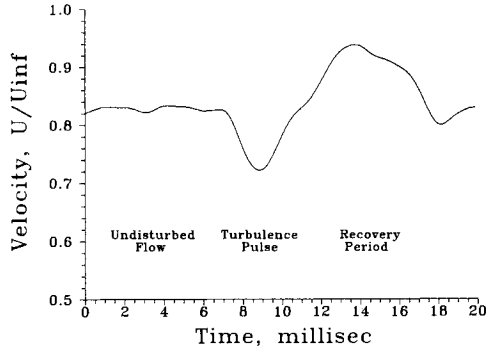

Fig. 5 Ensemble-averaged, low-pass filtered (smoothed) data, 70% chord.

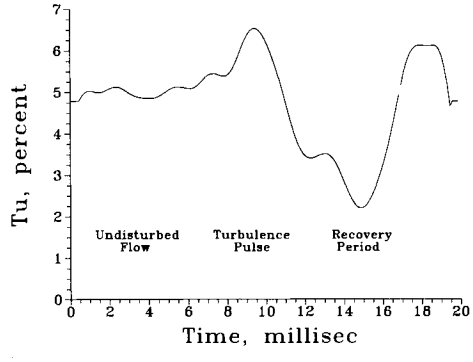

Fig. 6 Smoothed turbulence intensities for sample care.

To achieve a nonstationary mean velocity, ensemble averaging is performed, and a low-pass digital filter is applied by frequency domain smoothing. A smoothing window size is specified in the filtering process, and results in a cutoff frequency F_c being applied to the time-dependent discrete data. A 75-point window was selected, giving a value of F_c of 360 Hz which was determined to be appropriate for these data, considering the low-frequency unsteadiness due to the repeated (and not identical) pulse passage and the expected frequencies in transitional and turbulent boundary layers. The resulting smoothed and averaged data, for which the previous pulse was an example, are shown in Fig. 5. A parabolic filter was used in the frequency domain smoothing. For more information on the digital filtering process, see Ref. 7.

The fluctuating velocity component of the nonstationary flow is defined as the difference between the instantaneous velocity and the local smoothed velocity; the nonstationry mean is not ensemble averaged. This procedure prevents variations from pulse to pulse from being included incorrectly in the turbulence intensity. Smoothed intensities are shown in Fig. 6 for the sample case. Values range from the undisturbed value of 5%, to a peak of about 6%, and then to a value of about 2% before returning to the nominal value. Changes in turbulence intensities will be considered later as a means of characterizing the unusual recovery regime.

30% Chord Location

Figure 7 shows a series of velocity and turbulence intensity profiles over a pulse cycle at the laminar boundary-layer position. Again, the velocity is made dimensionless by the free-stream value rather than the time-dependent edge value. Note that the velocity abscissa in the upper plots are not plotted to zero. The undisturbed profile seen at the far left is laminar, with a thickness of about $y/c = 0.006$. The full effect of the turbulent pulse can be seen at 5.5 ms, with a much thicker boundary layer and a constant value of Tu across the layer of about 9%. As the pulse passes, the velocity profile shape and the level of turbulence return to the undisturbed values. No more will be presented of the laminar case, as it has been previously documented.[3,4]

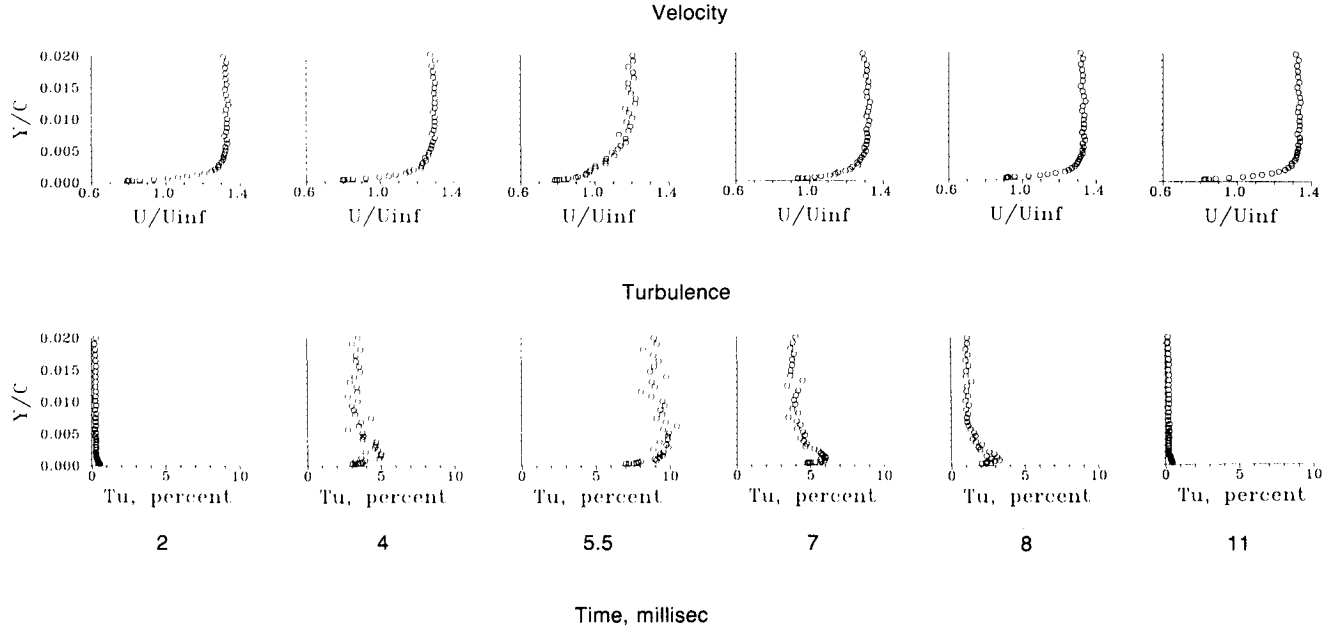

Fig. 7 Velocity and intensity profiles, 30% chord.

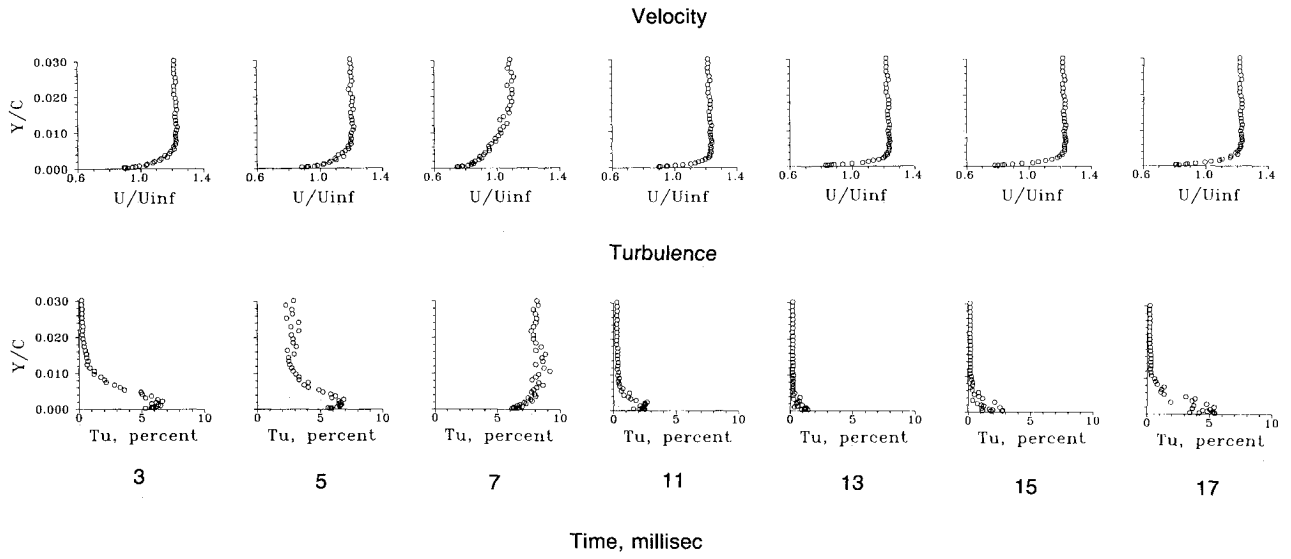

Fig. 8 Velocity and intensity profiles, 50% chord.

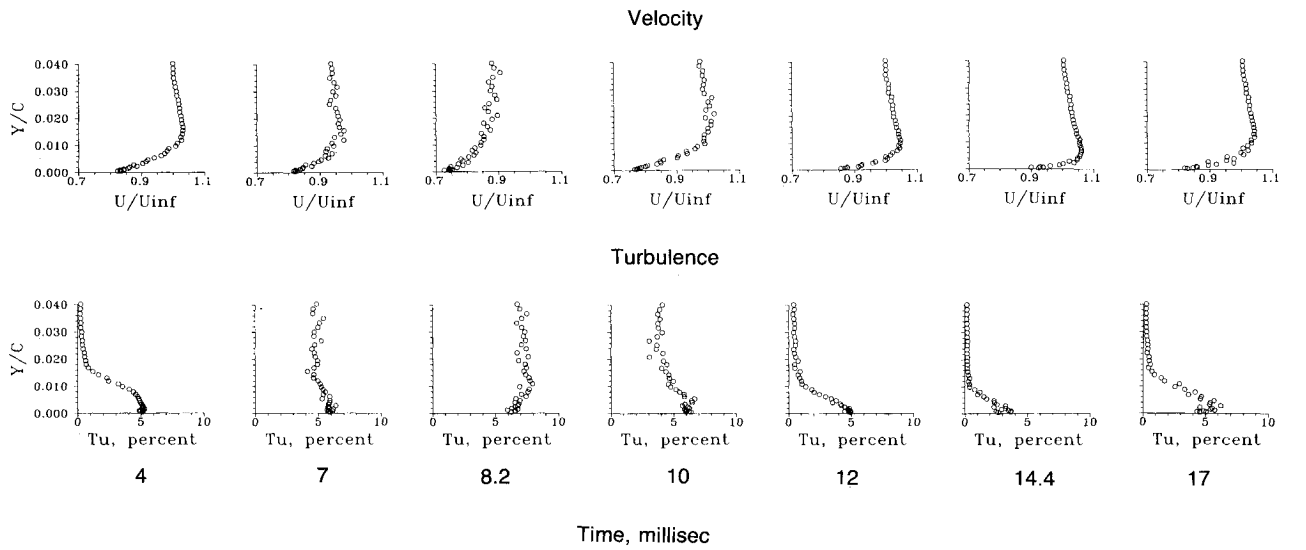

Fig. 9 Velocity and intensity profiles, 70% chord.

50% Chord Location

Velocity and *Tu* profiles for the transitional condition across a pulse cycle are shown in Fig. 8. The velocity profile shape and the 6% turbulence generated near the wing surface seen in the first frames (3 ms) indicate a transitional or near-turbulent boundary layer. The responses to the pulse are noted at 7 ms, similar to those for 30% chord, as the velocity profile becomes three times as thick and the intensity increases to over 8%, becoming constant across the layer.

The response seen at 13 ms is noteworthy. The boundary-layer thickness has decreased to about half of its undisturbed (transitional) value, and the turbulence intensity has reduced to barely 1% near the wall. A return to the undisturbed state is taking place by 17 ms. The stabilizing effect of the propeller slipstream disturbance noted in Ref. 3 is seen to exist also when caused by a disturbance with no thrusting component. The laminarization seen at 13 ms is brought on entirely as a result of the passage of an extremely highly turbulent wake-type disturbance in the external flow. To avoid repetition, spectral analysis will be presented only for the 70% chord case. For a discussion of the turbulence spectra for this transitional case, see Ref. 8.

70% Chord Location

Velocity and turbulence intensity profiles for a pulse cycle at the turbulent boundary-layer location are shown in Fig. 9. As seen in the first frames, the boundary layer is highly turbulent with a thickness of about $y/c = 0.015$ and an intensity of about 5% through most of the layer. The profile shape becomes much steeper as the pulse passes (8.2 ms), and the intensity reaches a constant value across the layer of about 7%. In the recovery region (14.4 ms), the turbulence intensity has been reduced to values much less than those for the undisturbed state (to a maximum of about 3%), and the boundary layer has decreased in thickness to 40% of the undisturbed value. The stabilizing mechanism works to return the boundary layer to a laminar-like condition, resulting in a velocity time history as shown in Fig. 4.

Ensemble-averaged velocity time histories at three locations in the boundary layer are shown in Fig. 10. The velocity deficit increases in midlayer and decreases as the surface is approached. Even very near the surface, a deficit of 20% of the undisturbed velocity takes place. Near the surface and in the midlayer, an acceleration after the passage of the turbulence pulse takes the local velocity to a level 7.5% higher than the

undisturbed value. It is this acceleration, brought about by the rapid transfer of momentum through the boundary layer, that may be responsible for the laminarization. The turbulent energy appears to provide the mechanism to stabilize the flow near the wing surface.

Spectral analysis was done on a selectable 256-point window of points across the pulse cycle, using a fast Fourier transform. Windows were taken for the undisturbed flow, the turbulence pulse, and for the recovery period, as shown in Figs. 11-13 for the 70% chord case. The nonstationary mean has been removed for all velocity spectra and total power plots. Spectra and power plots are shown for the same three locations in the boundary layer as for the time histories.

Figure 11 shows the frequency spectra very near the surface at $y/c = 0.00048$. The spectra indicate that the turbulence pulse and recovery period are dominated by low-frequency energy, whereas the undisturbed (nominally turbulent) flow has a slightly broader energy band. As 0 dB represents the highest magnitude frequency component in the flow region (here the pulse frequency), there is no information about the absolute power level in comparing the frequency plots. This information is given in the total (cumulative) power plots following the frequency plots.

In Fig. 12 at $y/c = 0.0082$, the response is similar to that nearer the surface. A significant difference can be noted in the external flow in Fig. 13 at $y/c = 0.0349$. The energy content for the undisturbed flow, as would be expected, is no longer dominated by turbulence and is almost indistinguishable from that for the recovery period.

The total power distribution plots give the turbulent power integrated over all frequencies. The results for the three boundary-layer locations are shown in Fig. 14. The labels for the three flow conditions are given in the middle graph.

Near the surface at $y/c = 0.00048$, there is a slight increase of half an order of magnitude in the turbulent power level when the turbulent pulse passes. The level remains high throughout the time cycle, and the undisturbed flow and recovery period contain identical cumulative power levels. The flow near the surface sees a slight rise in power due to the turbulent pulse, but otherwise the only change is in the frequency range of the turbulence, as noted by the higher power content at low frequencies for the recovery period.

At $y/c = 0.0082$, a significant difference in the total power levels for three flow conditions occurs. The turbulent power in the turbulence pulse is about 20 times larger than that in the undisturbed (nominally turbulent) flow, but the power content in the recovery period is not only 1/1000 that for the pulse but also 1/25 that of the undisturbed flow. This power difference is the distinguishing characteristic of the stabilizing effect of the time-dependent external turbulent-wake disturbance.

Outside of the boundary layer at $y/c = 0.0349$, the power levels for the undisturbed flow and the recovery period reach identical low values. There is a rise of three orders of magnitude as the turbulence pulse passes, but in the external flow, there is no noticeable difference between the recovery and undisturbed regions.

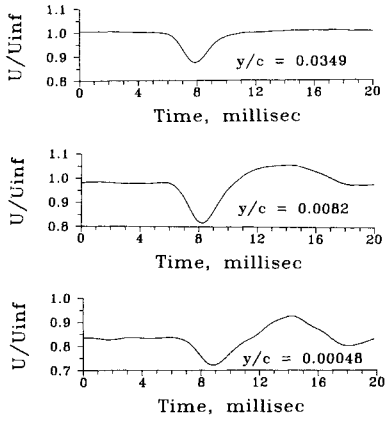

Fig. 10 Ensemble-averaged time histories in boundary layer, 70% chord.

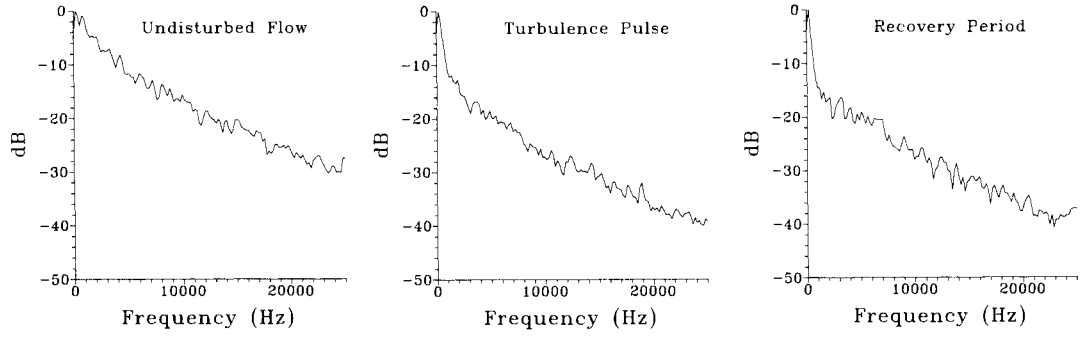

Fig. 11 Frequency spectra of turbulence, 70% chord, $y/c = 0.00048$.

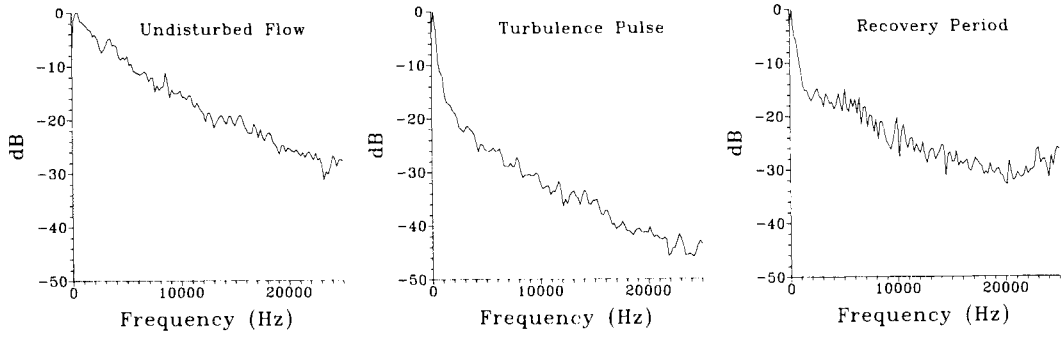

Fig. 12 Frequency spectra of turbulence, 70% chord, $y/c = 0.0082$.

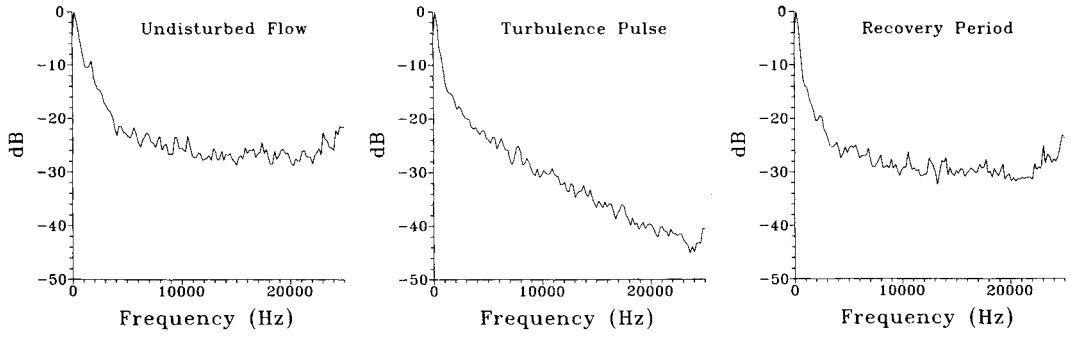

Fig. 13 Frequency spectra of turbulence, 70% chord, $y/c = 0.0349$.

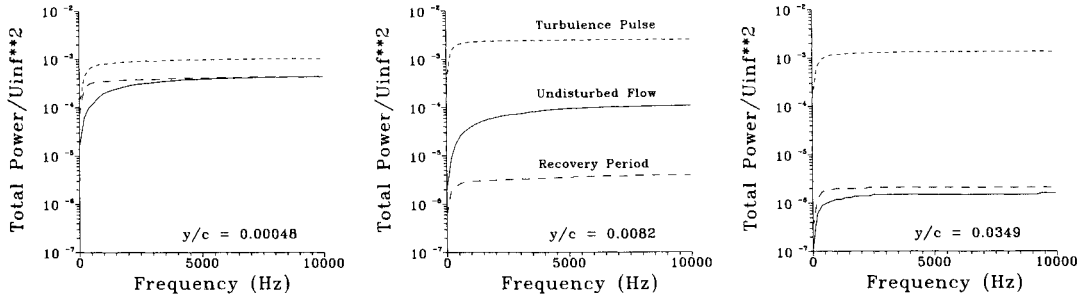

Fig. 14 Cumulative power across boundary layer, 70% chord.

Laminarization

The process of a turbulent boundary layer reverting to a laminar one has been studied if not well understood since the 1950s; a recent review of the various mechanisms responsible for the phenomenon was given by Narasimha and Sreenivasan.[9] Highly accelerating flows are one means to bring about this process. One of the most widely used parameters to predict the occurrence of laminarization is the acceleration parameter K:

$$K = \nu(\mathrm{d}U/\mathrm{d}x)/\bar{U}^2 \qquad (1)$$

An accepted value for reversion to take place is for K to be greater than 2 to 3.5×10^{-6}. In this form, it can be seen that no reliance is placed upon the local behavior inside the boundary layer; only the external flow velocity and its streamwise gradient are used for prediction. In some cases, integrated profile parameters, like momentum thickness and shape factors, are used to characterize the laminarizing behavior, as noted by Launder[10] and by Howard[6] with the data of Kline et al.[11] An attempt was made to apply the criterion locally inside the boundary layer to see if the correlation might hold.

At the 50% chord position, local accelerations due to the velocity deficit were on the order of 2500 to 3000 m/s^2. Near the airfoil surface, using a local mean velocity, a K value of 2.2×10^{-6} was determined; in the outer region, the value was 1.7×10^{-6}. At 30% chord, across the boundary layer the value held constant at 4.4×10^{-6}, but the boundary layer was returning to the laminar condition anyway. At 70% chord, K ranged from 1.3 to 1.9×10^{-6}. These values are marginally acceptable to predict laminarization, but it appears that the commonly used acceleration parameter also might be used for a time-dependent local acceleration of a boundary layer. This acceleration still may not be sufficient to describe the stabilizing mechanism, which involves the transfer of turbulent momentum downward to the airfoil surface and its quick removal. Three-dimensional effects also could possibly play a part. As Launder[10] notes, a true understanding of the laminarization phenomenon requires a knowledge of changes in the intensity, structure, and correlation of the turbulence and, in this case, in its time-dependent passage.

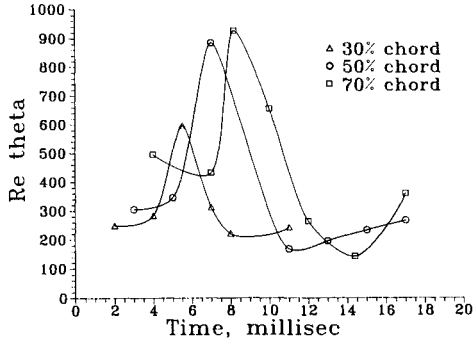

Fig. 15 Momentum-thickness Reynolds number time histories.

Momentum Thickness Reynolds Number

Boundary-layer behavior is frequently correlated with the momentum-thickness Reynolds number Re_θ. The momentum thickness is a measure of the local drag of the surface; Re_θ is often used to predict transition in a wall-bounded flow. Changes in Re_θ would tend to indicate any stabilizing influence of the time-dependent disturbance. It was of interest whether, at a fixed chord location, the value of Re_θ would cycle through a range of values, which would be expected if the boundary layer actually cycled between laminar-like, transitional, and turbulent conditions.

The ensemble-average velocity profiles were smoothed, fit with cubic splines, and integrated for values of Re_θ. Figure 15 shows the time histories for the three chord locations. The time can be correlated with the profiles in Figs. 7-9. In each case, and most notably for the 70% chord location, the value of Re_θ rises sharply at the passage of the turbulence pulse and returns to the undisturbed value after passing through a low value in the recovery region. The indication is that the passage of the turbulent-wake pulse serves to relaminarize the flow, even at 70% chord, where laminar flow could not be expected for conventional flow over the airfoil. The results confirm

what was seen in oscilloscope traces of the flow at 80% chord in Ref. 3.

Conclusions

The time-dependent boundary-layer response to a periodic turbulent flowfield has been studied for attached flow over an airfoil at laminar, transitional, and turbulent conditions. Hot-wire velocity measurements were made for nonstationary mean velocity and turbulence intensity profiles and for power spectra and cumulative power spectra plots.

The passage of a highly turbulent wake-flow pulse was found to have a stabilizing effect on the transitional and turbulent boundary layers. After the passage of the pulse, characterized by an increased profile thickness and a constant level of increased turbulence across the layer, the boundary layer passed through a recovery period in which the thickness was reduced to about half of its undisturbed value and the turbulence intensity to laminar-like conditions. The flow appears to undergo a laminarizing process before returning to its undisturbed (transitional or turbulent) state.

The laminarization of a turbulent boundary layer by the passage of a highly turbulent pulse is caused by a mechanism inherent in the time-dependent wake and not by any thrusting mechanism associated with a propeller flowfield.

The application of a commonly used acceleration parameter appears to correlate the occurrence of laminarization with the flow conditions in an unsteady environment as well as in a steady accelerating one. However, it is not known whether the acceleration mechanism is the sole cause or in fact the primary one in the stabilizing situation; the turbulence level itself also may play an important role.

Subsequent work will consider the effect of the unsteady turbulent input on incipient separation in an attempt to understand the effect of the stabilizing nature on flows near separation. A question to be considered is whether the stabilizing effect can be worked to an advantage in control at high angles of attack.

Acknowledgments

The support of the Aircraft Division, Research and Technology, Naval Air Systems Command, under the supervision of Thomas Momiyama and Harry Berman is gratefully acknowledged. This work is part of the research initiative on Enhanced Fighter Maneuverability. Thanks are given to Don Harvey for his excellent craftsmanship in machining the model supports and the rotating apparatus. Lastly, the authors wish to thank the reviewers and the associate editor for their helpful suggestions and comments.

References

[1]Carr, L. W., "Progress in Analysis and Prediction of Dynamic Stall," *Journal of Aircraft*, Vol. 25, No. 1, 1988, pp. 6-17.

[2]Brendel, M., "Experimental Study of the Boundary Layer on a Low Reynolds Number Airfoil in Steady and Unsteady Flow," Ph.D. Dissertation, Univ. of Notre Dame, Notre Dame, IN, May 1986.

[3]Miley, S. J., Howard, R. M., and Holmes, B. J., "Wing Laminar Boundary Layer in the Presence of a Propeller Slipstream," *Journal of Aircraft*, Vol. 25, No. 7, 1988, pp. 606-611.

[4]Howard, R. M., and Miley, S. J., "Time-Dependent Boundary Layer Response in a Propeller Slipstream," *Journal of Aircraft*, Vol. 26, No. 9, 1989, pp. 863-869.

[5]Kindelspire, D. W., "The Effects of Freestream Turbulence on Airfoil Boundary Layer Behavior at Low Reynolds Numbers," Masters Thesis, Naval Postgraduate School, Monterey, CA, Sept. 1988.

[6]Howard, R. M., "An Investigation of the Effects of the Propeller Slipstream on a Wing Boundary Layer," Ph.D. Dissertation, Texas A&M University, College Station, TX, May 1987.

[7]Johnson, D. K., "A Data Analysis System for Unsteady Turbulence Measurements," Masters Thesis, Naval Postgraduate School, Monterey, CA, Sept. 1988.

[8]Howard, R. M., and Renoud, R. W., "Wing Boundary Layer Response to an Unsteady Turbulent Flowfield," AIAA Paper 89-2226, July 1989.

[9]Narahimsa, R., and Sreenivasan, K., "Relaminarization of Fluid Flows," *Advances in Applied Mechanics*, Vol.19, 1979, pp. 221-309.

[10]Launder, B. E., "Laminarization of the Turbulent Boundary Layer in a Severe Acceleration," *Journal of Applied Mechanics*, Vol. 31, Series E, No. 4, Dec. 1964, pp. 707-708.

[11]Kline, S. J., Cantwell, B. J., and Lilley, G. M. (eds.), *The 1980-81 AFOSR-HTTM-Stanford Conference on Complex Turbulent Flows: Comparison of Computation and Experiment*, Mechanical Engineering Dept., Stanford Univ., Stanford, CA, Vol. 1, 1981, pp. 567-578.